Temperature dependence of avalanche multiplication in submicron Al 0.6 Ga 0.4 As diodes

C. N. Harrison, J. P. R. David, M. Hopkinson, and G. J. Rees

Citation: Journal of Applied Physics **92**, 7684 (2002); doi: 10.1063/1.1524017
View online: http://dx.doi.org/10.1063/1.1524017
View Table of Contents: http://scitation.aip.org/content/aip/journal/jap/92/12?ver=pdfcov
Published by the AIP Publishing

Temperature dependence of avalanche multiplication in submicron $Al_{0.6}Ga_{0.4}As$ diodes

C. N. Harrison,[a] J. P. R. David, M. Hopkinson, and G. J. Rees
Department of Electronic and Electrical Engineering, University of Sheffield, Sheffield, S1 3JD, United Kingdom

(Received 23 July 2002; accepted 4 October 2002)

Photomultiplication measured in $Al_{0.6}Ga_{0.4}As$ p^+-i-n^+ diodes falls with temperature in a manner that becomes less marked with decreasing *i*-region width and increasing electric field. Simple arguments relate this result to the effects of the ionization dead space, which is expected to depend weakly on temperature, and to the reduced scattering in the high electric fields present in thin avalanching structures. The temperature dependence of the ''enabled'' ionization coefficient can be approximately accounted for by simply subtracting the ballistic dead space from the width of the avalanche region. The simple arguments suggest the effect is independent of materials system. © *2002 American Institute of Physics.* [DOI: 10.1063/1.1524017]

Avalanche multiplication and breakdown increasingly limit the performance of high-power and microwave transistors as device dimensions continue to shrink and fields to increase. The avalanche process is conventionally characterized by the impact ionization coefficients for electrons, α, and holes, β, which depend on the local electric field and represent the inverse mean distance between ionization events. In many devices with high-field regions significantly shorter than 1 μm, carriers spend an appreciable fraction of this distance in acquiring energy from the field. The dead space, the distance over which the ionization coefficient achieves equilibrium with the electric field, then becomes a significant fraction of the multiplication width. Plimmer *et al.*[1] demonstrated the effect on multiplication in submicron GaAs diodes and the effects have since been observed in other material systems.[2]

Small, high-power devices, in which dead space effects are likely to be important, operate at elevated temperatures. Di Carlo and Lugli[3] showed that ignoring the dead space, *d*, given in the ballistic approximation by

$$d=\frac{E_{\mathrm{th}}}{q\xi}, \tag{1}$$

where E_{th} is the threshold energy for ionization, ξ is the electric field, and q is the electron charge, can result in an overestimate of the multiplication and an underestimate of the breakdown voltage. Dead space effects have also been shown to reduce the excess noise in thin avalanche structures.[4,5]

The impact ionization process is strongly temperature sensitive. The phonon population, and with it the carrier–phonon scattering rate, increase with temperature. The effect serves to cool the electron (hole) gas heated in the electric field, suppressing impact ionization and avalanche multiplication. However, the temperature dependence of impact ionization has been studied only in bulk structures, where the effects of dead space have not been considered.[6–8]

We report the temperature dependence of avalanche multiplication in submicron $Al_{0.6}Ga_{0.4}As$ p^+-i-n^+ diode structures at temperatures between 13 and 290 K. $Al_xGa_{1-x}As$ is used as a barrier region in field-effect transistors and as a collector in heterojunction bipolar transistors, where it is subject to high electric fields. This particular composition of $x=0.6$ was chosen because α and β are almost equal, even at low fields, allowing simple interpretation of the results.

A series of $Al_{0.6}Ga_{0.4}As$ p^+-i-n^+ structures with nominal *i*-region thicknesses, $w=0.05$, 0.1, and 0.8 μm, were grown epitaxially by molecular-beam epitaxy. Circular mesa diodes of diameter 100–400 μm, with annular top contacts for optical access, were fabricated using wet-chemical etching. Measurements of pure electron-initiated photomultiplication, M_e versus bias were made down to 13 K by focusing the light from an Ar^+ ion laser onto the top p^+ layers of the mesas to generate minority electrons. The optical excitation was chopped mechanically and the resulting ac signal was measured using a lock-in amplifier to distinguish the ac photocurrent from dc leakage currents. Measurements of both pure-electron- and pure-hole-initiated multiplication are usually needed on the same device to deduce α and β independently. However, since $\alpha\approx\beta$ in $Al_{0.6}Ga_{0.4}As$,[9] the effective ionization coefficients can be calculated from measurements of M_e alone, using a local model,[10] which ignores dead space effects. Then,

$$\alpha(=\beta)=\frac{M_e-1}{wM_e}, \tag{2}$$

where we have assumed equal local ionization coefficients and a constant electric field across the intrinsic region.

Figure 1 shows a typical dark current characteristic for the $w=0.05$ μm device as a function of reverse bias at 200 K. Note current is still less than 30 nA just below breakdown. The photocurrent characteristics shown were obtained from three separate devices with differing excitation powers. The slight linear increase at low bias, due to the improved

[a]Electronic mail: c.n.harrison@sheffield.ac.uk

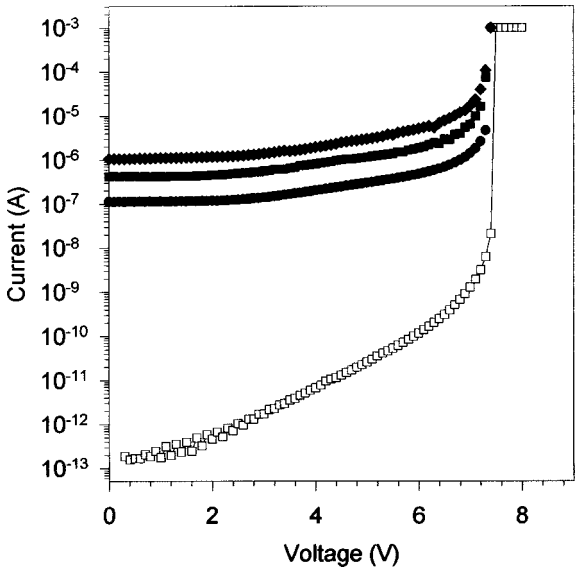

FIG. 1. Typical dark current (open symbols), and photocurrent characteristics of three different devices (closed symbols) for the $w=0.05$ μm layer at 200 K.

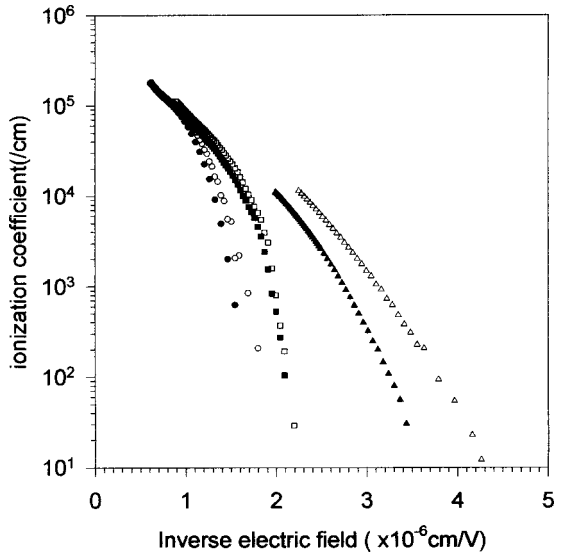

FIG. 3. Ionization coefficients at different temperatures vs inverse electric field for $w=0.05$ μm at 13 and 290 K (○, ●), 0.1 μm at 13 and 290 K (□, ■), and 0.8 μm at 13 and 290 K (△, ▲).

collection efficiency associated with the widening depletion layer, was corrected for when calculating M_e.[11]

Figure 2 shows M_e at temperatures between 13 and 290 K for diodes with three different *i*-region thicknesses. As expected, an increase in temperature suppresses multiplication in all devices and increases the breakdown voltage. However, it can be seen that the temperature dependence is significantly reduced for the thinnest device, making it difficult to distinguish the individual multiplication curves.

Figure 3 shows effective ionization coefficients as a function of inverse electric field for all three thicknesses. As expected from the multiplication characteristics, the ionization coefficients decrease with temperature, although only the 13 and 290 K coefficients are shown for clarity. The effective ionization coefficients, deduced on a local model from the multiplication curves using Eq. (2), appear to converge to values common to all lengths of device at high fields. However, at the lower fields, and in the thinner devices, where dead space effects are more significant, multiplication is suppressed and the values of the ionization coefficient lie below those deduced from measurements on the thicker devices, as seen elsewhere.[9] At 13 K the effective ionization coefficients in the thickest structure are appreciably larger than their room-temperature values, particularly at low fields, as expected. In the thinner devices, however, the increase is much smaller and the effective ionization coefficient is relatively unchanged.

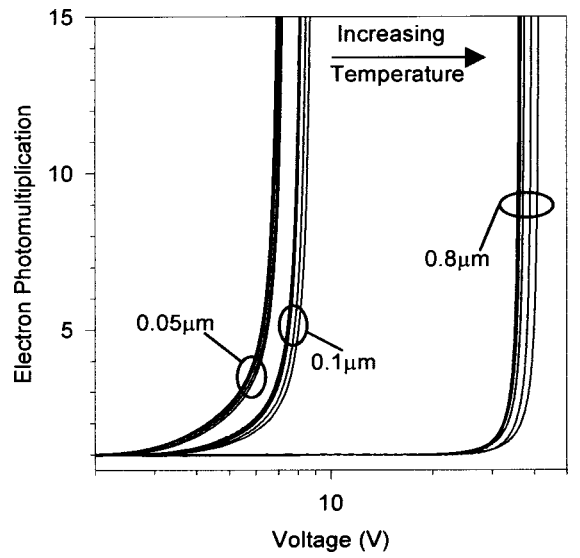

FIG. 2. Variation of M_e with temperature (13, 20, 50, 77, 120, 200, and 290 K) for the $w=0.05$, 0.1, and 0.8 μm diodes.

Inelastic carrier scattering in the high-field region is dominated by energy and momentum exchange with LO phonons, whose population is given by

$$n=\left[\exp\left(\frac{\hbar\omega}{kT}\right)-1\right]^{-1}, \tag{3}$$

where $\hbar\omega$ is the phonon energy, T is the absolute temperature, and k is Boltzmann's constant. The temperature dependence of Eq. (3) dominates that of ionization in thick devices, where the ionization coefficients are always close to equilibrium with the local electric field. In thin devices, operating at higher electric fields, carriers acquire the ionization threshold energy sooner, scattering from fewer phonons on the way, and the temperature dependence of the ionization coefficient is, consequently, reduced.

Furthermore, in thin devices, where the dead space is a significant fraction of the device width and of the ionization path length, the latter quantity is not exponentially distributed (as in the local model). Monte Carlo simulations[12] show a significant peak in the ionization path length distribution after a distance d, given by Eq. (1). This ballistic model provides a good description of dead space in this situation since, although a carrier may have scattered many times before acquiring threshold energy, the net energy exchanged

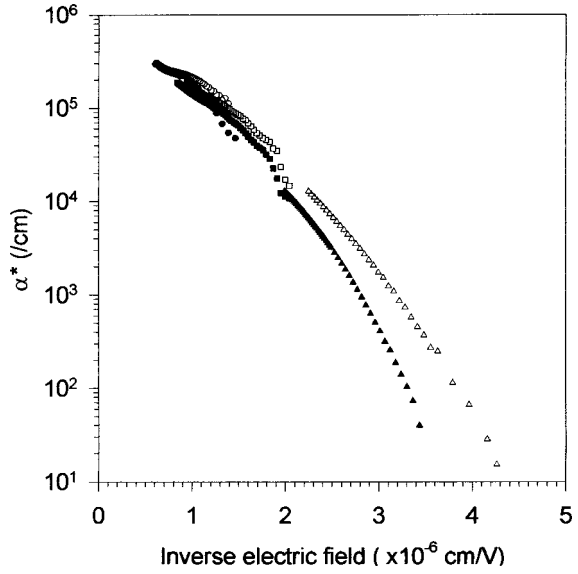

FIG. 4. α^* vs inverse electric field for $w=0.05$ μm at 13 and 290 K (○, ●), 0.1 μm at 13 and 290 K (□, ■), and 0.8 μm at 13 and 290 K (△, ▲).

with the lattice via phonon absorption and emission processes is small compared with E_{th} ($\sim$ several eV) since $\hbar\omega$ is small (typically, 30 meV).

In fact, multiplication and noise can be described well in this nonlocal regime by a displaced exponential ionization path length probability distribution function (pdf).[12] In this model the ionization path length is equal to zero within a ballistic dead space of generating a carrier and is, subsequently, distributed as a decaying exponential with an inverse decay length given by the ''enabled'' ionization coefficient, α^* or β^*.[13] Whereas this ballistic dead space is not sensitive to temperature, we can expect the enabled ionization coefficients to exhibit the temperature dependence of the conventional, local ionization coefficients, α and β, to which they collapse in the local limit.

To extract the temperature dependence of α^* $(=\beta^*)$ we would need to fit the curves of Fig. 2 to the predictions of nonlocal multiplication models,[14,15] using a displaced exponential model for the ionization path length pdf. Instead, we can use a simpler, approximate technique, following Bulman, Robbins, and Stillman,[16] and suppose that the effect of dead space is to reduce avalanche region width w by d so that Eq. (2) now evaluates the enabled ionization coefficients,

$$\alpha^*(=\beta^*)=\frac{M-1}{(w-d)M}. \tag{4}$$

The results of this exercise are displayed in Fig. 4, which shows the enabled ionization coefficients versus inverse electric field for the range of device widths at the two extreme temperatures. The results for different device widths at the same temperature fall on approximately the same curve, suggesting that we have accounted reasonably well for the effects of dead space in this approximate treatment. The temperature dependencies are also in line with the behavior expected for thick devices with local behavior.

The simple arguments used to explain this behavior are largely material independent. Consequently, the multiplication characteristics of submicron avalanching regions can be expected to be largely temperature independent as a result of the reduced scattering in the higher electric fields and increased importance of the dead space.

This work was supported by EPSRC UK.

[1] S. A. Plimmer *et al.*, IEEE Trans. Electron Devices **43**, 1066 (1996).
[2] S. A. Plimmer, J. P. R. David, R. Grey, and G. J. Rees, IEEE Trans. Electron Devices **47**, 1089 (2000).
[3] A. Di Carlo and P. Lugli, IEEE Electron Device Lett. **14**, 103 (1993).
[4] C. Hu, K. A. Anselm, B. G. Streetman, and J. C. Campbell, Appl. Phys. Lett. **69**, 3734 (1996).
[5] K. F. Li, D. S. Ong, J. P. R. David, G. J. Rees, R. C. Tozer, P. N. Robson, and R. Grey, IEEE Trans. Electron Devices **45**, 2102 (1998).
[6] X. G. Zheng, P. Yuan, X. Sun, G. S. Kinsey, A. L. Holmes, B. G. Streetman, and J. C. Campbell, IEEE J. Quantum Electron. **36**, 1168 (2000).
[7] F. Osaka and T. Mikawa, J. Appl. Phys. **58**, 4426 (1985).
[8] M. R. Brozel and G. E. Stillman, IEE Emis Datareviews Series, 3rd ed., No. 16, 1996, Chap. 4.9D, p. 195.
[9] C. H. Tan, J. P. R. David, S. A. Plimmer, G. J. Rees, R. C. Tozer, and R. Grey, IEEE Trans. Electron Devices **48**, 1310 (2001).
[10] G. E. Stillman and C. M. Wolfe, *Semiconductors and Semimetals* (Academic, New York, 1977), Vol. 12, p. 291.
[11] M. H. Woods, W. C. Johnson, and M. A. Lampert, Solid-State Electron. **16**, 381 (1973).
[12] D. S. Ong, K. F. Li, G. J. Rees, G. M. Dunn, J. P. R. David, and P. N. Robson, IEEE Trans. Electron Devices **45**, 1804 (1998).
[13] R. J. McIntyre, IEEE Trans. Electron Devices **46**, 1623 (1999).
[14] D. S. Ong, K. F. Li, G. J. Rees, J. P. R. David, and P. N. Robson, J. Appl. Phys. **83**, 3426 (1998).
[15] M. M. Hayat, B. E. A. Saleh, and M. C. Teich, IEEE Trans. Electron Devices **ED-39**, 546 (1992).
[16] G. E. Bulman, V. M. Robbins, and G. E. Stillman, IEEE Trans. Electron Devices **ED-32**, 2454 (1985).